Chiral Control in the Staudinger Reaction between Ketenes and Imines. A Theoretical SCF-MO Study on Asymmetric Torquoselectivity

Fernando P. Cossío,*,† Ana Arrieta,† Begoña Lecea,‡ and Jesus M. Ugalde†

Contribution from the Kimika Fakultatea, Euskal Herriko Unibertsitatea, P.K. 1072, 20080 San Sebastián-Donostia, Spain, and Farmazi Fakultatea, Euskal Herriko Unibertsitatea, Lasarteko Ataria z/g, 01007 Vitoria-Gasteiz, Spain

*Received June 21, 1993. Revised Manuscript Received November 5, 1993**

Abstract: The different modes of interaction between achiral ketenes and homochiral aldimines derived from chiral aldehydes to give the two possible diastereoisomers of *cis*-β-lactams have been examined using the AM1 method. It has been found that the step which determines the final stereochemistry is the conrotatory ring closure between C_3 and C_4 atoms. The high diastereoselectivity predicted by our calculations is in excellent agreement with available experimental data. The origin of this high stereocontrol is rationalized on the basis of the stabilizing interaction between the C–X σ* orbital (X being an electronegative atom) and the p atomic orbital of the C_3 atom. A similar treatment has been applied to the interaction between achiral imines and homochiral ketenes. Our calculations predict high diastereomeric excesses which again are in good agreement with the experimentally found diastereoselection.

Introduction

Since its discovery by Staudinger[1] in 1907, the interaction between ketenes and imines to form β-lactams (2-azetidinones) has been one of the most versatile and useful approaches to the synthesis of these compounds[2] and hence to the diverse families of β-lactam antibiotics,[3] as well as diverse, important natural products for which 2-azetidinones constitute key intermediates.[4]

Although the synthetic utility of the Staudinger reaction (SR) has been extensively explored, one of the most challenging goals currently under active research is the development of methodologies which lead to an effective chiral control in the formation of the corresponding β-lactam. This control can be induced from the four positions of the β-lactam ring.[5-8] One possibility consists of the interaction between achiral ketenes and imines derived from homochiral aldehydes, which constitutes at present one of the best methodologies in the chiral SR in terms of high diastereoselection and generality. The first synthesis using this approach was reported in 1983 by Hubschwerlen and Schmid.[9] These authors observed a complete diastereoselection in the reaction between monosubstituted ketenes and imines derived from (*S*)-glyceraldehyde acetonide (Scheme 1, entry a). In addition, other authors have reported related studies on this approach based on either D-glyceraldehyde acetonide or related chiral sources[10] and have described some interesting synthetic applications of the chiral β-lactams thus formed. Some research groups[11] have described the interaction between achiral ketenes and imines prepared using protected lactic and mandelic acids as chiral sources (Scheme 1, entry b). On the other hand, Evans and Williams[12] have reported a high induction in the SR between achiral ketenes and imines derived from chiral epoxy aldehydes, readily accessible from allyl alcohols *via* Sharpless asymmetric epoxidation (Scheme 1, entry c). This approach gives also a

† Kimika Fakultatea.

‡ Farmazi Fakultatea.

* Abstract published in *Advance ACS Abstracts*, January 15, 1994.

(1) Staudinger, H. *Liebigs Ann. Chem.* **1907**, *356*, 51.

(2) For recent reviews, see: (a) Ghosez, L.; Marchand-Brynaert, S. In *Comprehensive Organic Synthesis*; Trost, B., Fleming, I., Eds.; Pergamon: Oxford, 1991; Vol. 5, p 85. (b) Thomas, R. C. In *Recent Progress in The Chemical Synthesis of Antibiotics*; Lukacs, G., Ohno, M., Eds.; Springer-Verlag: Berlin, 1988; p 533. (c) van der Steen, F. H.; van Koten, G. *Tetrahedron* **1991**, *47*, 7503. (d) Georg, G. L.; Ravikumar, V. T. In *The Organic Chemistry of β-Lactams*; Georg, G. L., Ed.; Verlag Chemie: New York, 1993; pp 295–381. (e) Backes, I. In *Methoden der Organischen Chemie, Vol. E15b, Organische Stickstoffverbindungen II*; Klagman, D., Ed.; Georg Thieme: Stuttgart, 1991; pp 383–483.

(3) *Chemistry and Biology of β-Lactam Antibiotics*; Morin, R. B., Gorman, M., Eds.; Academic Press: New York, 1982; Vols. 1–3.

(4) (a) Manhas, M. S.; Amin, S. G.; Bose, A. K. *Heterocycles* **1976**, *5*, 699. (b) Manhas, M. S.; Wagle, D. R.; Chiang, J.; Bose, A. K. *Heterocycles* **1988**, *27*, 1755.

(5) (a) Ghosez, L.; Bogdan, S.; Cérésiat, M.; Frydrych, C.; Marchand-Brynaert, J.; Moya-Portuguez, M.; Hubert, I. *Pure Appl. Chem.* **1987**, *59*, 393. (b) Marchand-Brynaert, J.; Moya-Portuguez, M.; Hubert, I.; Ghosez, L. *J. Chem. Soc., Chem. Commun.* **1983**, 818. (c) Belzecki, C.; Rogalska, E. *J. Chem. Soc., Chem. Commun.* **1981**, 57. (d) Rogalska, E.; Belzecki, C. *J. Org. Chem.* **1984**, *49*, 1397.

(6) (a) Thomas, R. C. *Tetrahedron Lett.* **1989**, *30*, 5239. (b) Teutsch, G.; Bonnet, A. *Tetrahedron Lett.* **1984**, *25*, 1561. (c) Klich, M.; Teutsch, G. *Tetrahedron* **1986**, *42*, 2677. (d) Dugat, D.; Just, G.; Sahoo, S. *Can. J. Chem.* **1987**, *65*, 88. (e) Gunda, T. E.; Vieth, S.; Kövér, K. E.; Sztaricskai, F. *Tetrahedron Lett.* **1990**, *46*, 6707. (f) Aszodi, J.; Bonnet, A.; Teutsch, G. *Tetrahedron Lett.* **1990**, *46*, 1579.

(7) (a) Kamiya, T.; Oku, T.; Nakaguchi, O.; Takeno, H.; Hashimoto, M. *Tetrahedron Lett.* **1978**, *19*, 5119. (b) Bose, A. K.; Manhas, M. S.; Van der Veen, J. M.; Bari, S. S.; Wagle, D. R.; Hegde, V. R.; Krishnan, L. *Tetrahedron Lett.* **1985**, *26*, 33. (c) Belleau, B.; Tenneson, S. M. *Can. J. Chem.* **1980**, *58*, 1605. (d) Hashiguchi, S.; Maeda, Y.; Kishimoto, S.; Ochiai, M. *Heterocycles* **1986**, *24*, 2273. (e) Just, G.; Liak, T. *Can. J. Chem.* **1978**, *56*, 211. (e) Arrieta, A.; Lecea, B.; Cossío, F. P.; Palomo, C. *J. Org. Chem.* **1988**, *53*, 3784. (f) Nakaguchi, O.; Oku, T.; Takeno, H.; Hashimoto, M.; Kamiya, T. *Chem. Pharm. Bull.* **1987**, *35*, 3985. (g) Farina, V.; Hauck, S. I.; Walker, D. G. *Synlett* **1992**, 761. (h) Bose, A. K.; Manhas, M. S.; van der Veen, J.; Bari, S. S.; Wagle, D. *Tetrahedron* **1992**, *48*, 4831. (i) Banik, B. K.; Manhas, M. S.; Bose, A. K. *J. Org. Chem.* **1993**, *58*, 307.

(8) (a) Barton, D. H. R.; Gateau-Olesker, A.; Anaya-Mateos, J.; Cléophax, J.; Géro, S. D.; Chiaroni, A.; Riche, C. *J. Chem. Soc., Perkin Trans 1* **1990**, 3211. (b) Borer, B. C.; Balogh, D. W. *Tetrahedron Lett.* **1991**, *32*, 1039. (c) Georg, G. I.; Akgün, E.; Mashava, P. M.; Milstead, M.; Ping, H.; Wu, Z.; Vander Velde, D.; Takusagawa, F. *Tetrahedron Lett.* **1992**, *33*, 2111.

(9) Hubschwerlen, C.; Schmid, G. *Helv. Chim. Acta* **1983**, *66*, 2206.

(10) (a) Bose, A. K.; Manhas, M. S.; van der Veen, J. M.; Bari, S. S.; Wagle, D. R.; Hegde, V. R.; Krishnan, L. *Tetrahedron Lett.* **1985**, *26*, 33. (b) Bose, A. K.; Hegde, V. R.; Wagle, D. R.; Bari, S. S.; Manhas, M. S. *J. Chem. Soc., Chem. Commun.* **1986**, 161. (c) Wagle, D. R.; Garai, C.; Chiang, J.; Monteleone, M.; Kurys, B. E.; Strohmeyer, T. W.; Hegde, V. R.; Manhas, M. S.; Bose, A. K. *J. Org. Chem.* **1988**, *53*, 4227. (d) Banik, B. K.; Manhas, M. S.; Kaluza, Z.; Barakat, K. J.; Bose, A. K. *Tetrahedron Lett.* **1992**, *33*, 3603. (e) Welch, J. T.; Araki, K.; Kawecki, R.; Wichtowski, J. A. *J. Org. Chem.* **1993**, *58*, 2454.

(11) (a) Kobayashi, Y.; Takemoto, Y.; Ito, Y.; Terashima, S. *Tetrahedron Lett.* **1990**, *31*, 3031. (b) Kobayashi, Y.; Takemoto, Y.; Kamijo, T.; Harada, H.; Ito, Y.; Terashima, S. *Tetrahedron* **1992**, *48*, 1853. (c) Palomo, C.; Cossío, F. P.; Ontoria, J. M.; Odriozola, J. M. *Tetrahedron Lett.* **1991**, *32*, 3105. (d) Terashima, S. *Synlett* **1992**, 691.

(12) (a) Evans, D. A.; Willliams, J. M. *Tetrahedron Lett.* **1988**, *29*, 5065. (b) Frazier, J. W.; Staszak, M. A.; Weigel, L. O. *Tetrahedron Lett.* **1992**, *33*, 857.

0002-7863/94/1516-2085$04.50/0

Scheme 1

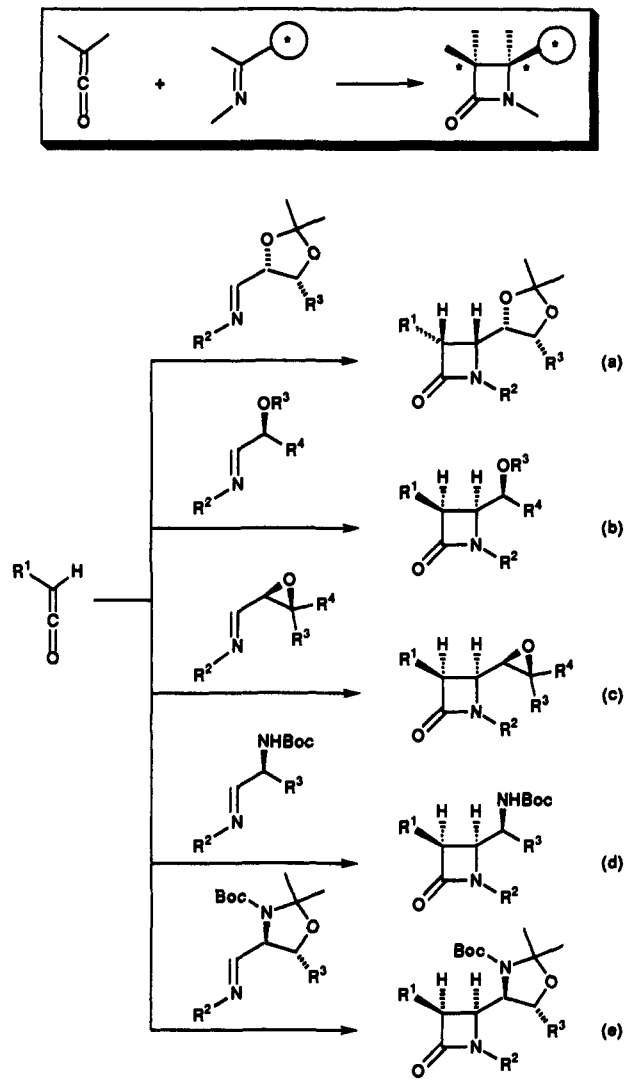

Scheme 2

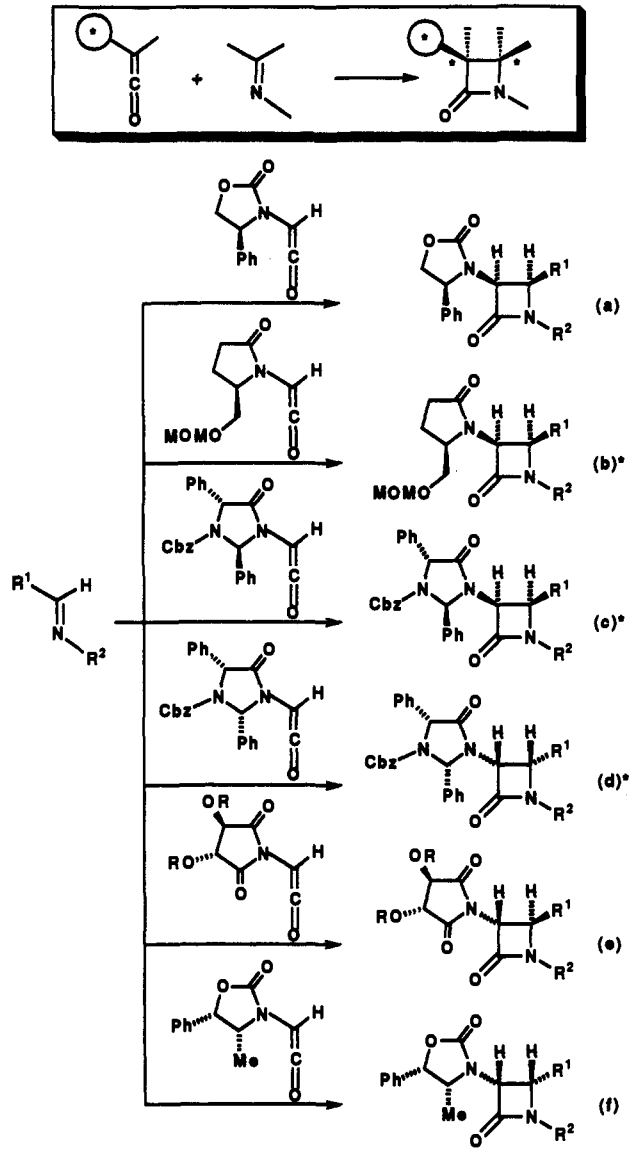

* Minor quantities of the *trans* isomer were also obtained

good stereocontrol, although somewhat lower than in the preceding cases. Finally, some recent papers from our laboratories[13] have reported the complete diastereoselection observed in the SR using imines derived from chiral α-amino aldehydes (Scheme 1, entries d and e). It is noteworthy that all of these methodologies lead to β-lactams which can be elaborated at the C_4 position to give useful precursors in the chemical synthesis of β-lactam antibiotics and/or interesting molecules such as amino acids, peptides, sugars, and pyrrolidin-2-ones.[4] Interestingly, all the reactions outlined in the Scheme 1 lead to β-lactams possessing the same stereochemical relationships, thus suggesting that the origins of the chiral control observed in these reactions must be similar in nature.

The alternative general methodology to obtain with a high level of stereoselection chiral β-lactams *via* the SR consists of the interaction between achiral imines and chiral ketenes. The first efficient materialization of this approach was published by Evans and Sjögren.[14] These authors described the reaction between achiral imines and the ketene derived from (4*S*)-phenyloxazolidinylacetyl chloride, prepared from readily available (*S*)-phenylglycine (Scheme 2, entry a). Several groups have studied extensively this methodology and applied it to the synthesis of diverse β-lactam antibiotics and related compounds[15,16] with excellent results in terms of generality and applicability. Other chiral ketenes have also been investigated. For instance, Ikota *et al.*[17] examined chiral ketenes derived from L-(+)-tartaric acid and (*S*)-serine (Scheme 2, entries b and c, respectively). However, in the former case the stereoselectivity was lower, giving *cis*/*trans* mixtures of the corresponding β-lactams, whereas in the latter case *trans* isomers were obtained with *ca.* 60% diastereomeric excess. Cooper *et al.*[18] found that a complementary chiral source with respect to the Evans–Sjögren ketenes is the ketene derived from norephedrine (Scheme 2, entry f). In this case, a small group such as methyl is enough to obtain excellent

(13) (a) Palomo, C.; Cossío, F. P.; Cuevas, C. *Tetrahedron Lett.* **1991**, *32*, 3109. (b) Palomo, C.; Cossío, F. P.; Cuevas, C.; Lecea, B.; Mielgo, A.; Román, P.; Luque, A.; Martinez-Ripoll, M. *J. Am. Chem. Soc.* **1992**, *114*, 9360.

(14) (a) Evans, D. A.; Sjögren, E. B. *Tetrahedron Lett.* **1985**, *26*, 3783. (b) Evans, D. A.; Sjögren, E. B. *Tetrahedron Lett.* **1985**, *26*, 3787.

(15) (a) Ojima, I.; Chen, H.-J. C. *J. Chem. Soc., Chem. Commun.* **1987**, 625. (b) Ojima, I.; Chen, H.-J. C.; Qiu, X. *Tetrahedron* **1988**, *44*, 5307. (c) Ojima, I.; Chen, H.-J. C.; Nakahashi, K. *J. Am. Chem. Soc.* **1988**, *110*, 278. (d) Jackson, B. G.; Gardner, J. P.; Heath, P. C. *Tetrahedron Lett.* **1990**, *31*, 6317. (e) Muller, M.; Bur, D.; Tschamber, T.; Streith, J. *Helv. Chim. Acta* **1991**, *74*, 767. (f) Boger, D. L.; Myers, J. B., Jr. *J. Org. Chem.* **1991**, *56*, 5385.

(16) (a) Ojima, I.; Shimizu, N.; Qiu, X.; Chen, H.-J. C.; Nakahashi, K. *Bull. Soc. Chim. Fr.* **1987**, 649. (b) Ojima, I.; Chen, H.-J. C.; Qiu, X. *Tetrahedron* **1988**, *44*, 5307.

(17) (a) Ikota, N.; Hanaki, A. *Heterocycles* **1984**, *21*, 418. (b) Ikota, N.; Shibata, H.; Koga, K. *Chem. Pharm. Bull.* **1985**, *33*, 3299. (c) Ikota, N. *Chem. Pharm. Bull.* **1990**, *38*, 1601.

(18) Cooper, R. D. G.; Daugherty, B. W.; Boyd, D. B. *Pure Appl. Chem.* **1987**, *59*, 485.

chiral induction. On the other hand, chiral ketenes derived from imidazolones prepared from (*R*)-phenylglycine resulted in good to low chiral inductions, depending upon the group R used (see Scheme 2, entries c and d). However, these chiral ketenes lead to variable quantities of the undesired *trans* isomers. More interesting is that the sense of induction is completely governed by the configuration at the carbon atom contiguous to the nitrogen of the ketene. Thus, in the entries c and d of Scheme 2, we can observe that the configurations at the C_3 and C_4 atoms of the β-lactams products are opposite each other, in spite of the same configuration of the carbon atom contiguous to the carbonyl group of the imidazolone group. Thus, this suggests that the factors that govern the stereochemical outcome in these cycloadditions should be the same, with the only exception being the ketenes derived from tartaric acid (Scheme 2, entry e), which lead only to the *trans* isomers.

In view of the above precedents and within the context of our interest in the study of the SR,[13b,19] it is the aim of this work to study from a theoretical standpoint the SR between achiral ketenes and chiral imines in which the chiral source is at the α-position of the C_{sp^2} atom of the imine, as well as the SR between achiral imines and chiral Evans–Sjögren and related ketenes. Our final goal has been to understand the origin of the exceptionally high chiral induction of these reactions.

Methods

The semiempirical SCF-MO AM1[21] method has been used throughout this work. Previous work from our laboratories[19] on more simple systems showed that the AM1/RHF method compares well with *ab initio* results, which must be performed at least at the HF/6-31G* level[20] to reproduce conveniently the profile of this reaction. Calculations were carried out with the standard parameters[21] using a locally modified version[22] of the MOPAC 6.0 package,[23] which includes the optimization algorithm described by Powell.[24] In a previous paper,[19] we studied the effect of including the molecular mechanics correction (MMOK keyword) in monocyclic β-lactams, and we found that in the case of *N*-methylazetidin-2-ones the effect of such a correction is negligible. In particular, the amidic N–C bond distance remains virtually unchanged. Therefore, since the SR includes the formation of the amidic N–C bond, the results reported here have been obtained specifying the NOMM option, in order to use an homogeneous treatment along the reaction path. Reactants, products, and reaction intermediates were optimized using the Broyden–Fletcher–Goldfarb–Shanno[25] (BFGS) geometry optimizer. The TSs were optimized using Powell,[24] Bartels,[26] McIver-Komornicki,[27] and eigenvector following[28] methods. All stationary points were refined by minimization of the gradient norm of the energy at least below 0.01 kcal/Å·deg and characterized by harmonic vibrational frequency analysis.[29] All reactants, intermediates, and products had positive, definite Hessian matrices, and the TSs showed only one negative eigenvalue in their diagonalized Hessians, corresponding to motion along the reaction coordinate. All calculations were performed with the more precise SCF convergence and minimization criteria, according to the recommendations of Boyd, Stewart, *et al.*[30] For a given substituent, the data reported refer to its most stable conformer, unless otherwise stated. Allowance for geometrical relaxation from the TSs after small geometrical distortions led in all cases to the local minima corresponding to the reactants, products, or reaction intermediates. Entropies were obtained from the calculated geometries and vibrational frequencies as previously described by Dewar *et al.*[31] The bond indexes[32] between atoms A and B were calculated as

$$B_{AB} = \sum_{\mu \in A} \sum_{\nu \in B} P_{\mu\nu}^2 \qquad (1)$$

where $P_{\mu\nu}$ are the elements of the density matrix and the subscripts μ and ν refer to atomic orbitals (AOs) centered at atoms A and B, respectively.

The SR is usually carried out in a limited range of solvents.[5-18] The more commonly used solvents are aromatic hydrocarbons (benzene, toluene) and dichloromethane or chloroform. It has been found that, in the range of polarities studied, the stereochemical outcome of the asymmetric SR is the same, thus suggesting that the reasons underlying in the asymmetric induction in these reactions must be independent of the nature of the solvent. Therefore, all the calculations presented in this work do not take into account solvent effects and correspond to the gas phase.

Results and Discussion

General Considerations. In a previous paper,[19] we discussed the nature of the factors that determine the stereochemical outcome of the SR. We concluded that the SR takes place in two steps, the former consisting of the nucleophilic attack of the nitrogen of the imine **2** over the carbonyl of the ketene **1** to form the zwitterionic intermediate **4**, whose thermal conrotatory electrocyclization yields the β-lactam product **6** (Scheme 3). Thus, the formation of a *cis*-β-lactam starting from an (*E*)-imine requires first the *exo* attack in the TS **3** and second the 3-out/4-in disposition of the substituents in the TS **5**.[19] Earlier work by Boyd *et al.*[18,33] showed that the first step of the SR takes place in a non-coplanar fashion, thus yielding two possible TSs **3** and two zwitterionic intermediates **4** (see Scheme 3). As a consequence, the formation of the C_3–C_4 bond *via* conrotatory cyclization implies not only torsion of the two π systems but also rotation around the N_1–C_2 bond. If we denote ω as the dihedral angle C_4–N_1–C_2–C_3 (see Figure 1), the sign of ω indicates the sense of rotation of C_4 around the N_1–C_2 bond to form the corresponding β-lactam ring, in which the value of ω is nearly 0. Hence, we have denoted the TSs **3** and the intermediates **4** as **P** when this rotation takes place in a clockwise sense and as **M** when the rotation around the N_1–C_2 bond is counterclockwise (Figure 1). Of course, an equilibration between the intermediates **4M** and **4P** can also occur (**4M** $\rightleftarrows$ **4P**), and it is expected that this equilibration must be faster than the formation of the C_3–C_4 bond. These two reaction paths lead to the two different TSs **5P** and **5M**, corresponding to the clockwise and counterclockwise possible conrotations, respectively (Scheme 3). Note as pointed out by Hegedus *et al.*[34] that the geometries indicated in Scheme 3 are those required to minimize the torsion around the two π systems, since closure in the opposite direction would necessitate the C_3 and C_4 substituents to pass through each other. When R^1 and R^2 are achiral, the two reaction paths are isoenergetic, but when R^1 and/or R^2 are chiral, unequal quantities of the *cis*-β-lactams **6P** and **6M** will be formed. According to the terminology recently introduced by Houk,[35] this second step leading to β-lactams **6** constitutes an interesting case of asymmetric torquoselectivity.

(19) Cossío, F. P.; Ugalde, J. M.; Lopez, X.; Lecea, B.; Palomo, C. *J. Am. Chem. Soc.* **1993**, *115*, 995.
(20) Sordo, J. A.; Gonzalez, J.; Sordo, T. L. *J. Am. Chem. Soc.* **1992**, *114*, 6249.
(21) (a) Dewar, M. J. S.; Zoebisch, E. G.; Healy, E. F.; Stewart, J. J. P. *J. Am. Chem. Soc.* **1985**, *107*, 3902. (b) Dewar, M. J. S.; Jie, C. *Organometallics* **1987**, *6*, 1486.
(22) Olivella, S. *QCPE Bull.* **1984**, *9*, 10 (extended by Olivella, S.; Bofill, J. M., 1990). The implementation of the Powell optimizer (see ref 24) in this version allows a fast localization characterization of stationary points, which can then be refined using standard procedures. The stationary points thus located do not differ from the ones obtained by using the "official" release of MOPAC 6.0.
(23) (a) Stewart, J. J. P. *QCPE Bull.* **1983**, *3*, 101. (b) *QCPE* 455. Indiana University, Bloomington, IN.
(24) Powell, M. J. D. In *Numerical Methods for Nonlinear Algebraic Equations*; Rabinowitz, P., Ed.; Gordon Breach: New York, 1970.
(25) (a) Broyden, C. G. *J. Inst. Math. Its Appl.* **1970**, *6*, 222. (b) Fletcher, R. *Comput. J.* **1970**, *13*, 317. (c) Goldfarb, D. *Math. Comput.* **1970**, *24*, 23. (d) Shanno, D. F. *Math. Comput.* **1970**, *24*, 647.
(26) Bartels, R. H. Report CNA-44; University of Texas; Center for Numerical Analysis: Austin, TX, 1972.
(27) (a) Komornicki, A. K.; McIver, J. W. *Chem. Phys. Lett.* **1971**, *10*, 303. (b) Komornicki, A. K.; McIver, J. W. *J. Am. Chem. Soc.* **1972**, *94*, 2625.
(28) Baker, J. *J. Comput. Chem.* **1986**, *7*, 385.
(29) McIver, J. W.; Komornicki, A. K. *J. Am. Chem. Soc.* **1972**, *94*, 2625.
(30) Boyd, D. B.; Smith, D. W.; Stewart, J. J. P.; Wimmer, E. *J. Comput. Chem.* **1988**, *9*, 387.
(31) Dewar, M. J. S.; Ford, G. P. *J. Am. Chem. Soc.* **1977**, *99*, 7822.
(32) Wiberg, K. B. *Tetrahedron* **1968**, *24*, 1083.
(33) Boyd, D. B. Computer-Assisted Molecular Design Studies of β-Lactam Antibiotics. In *Frontiers on Antibiotic Research*; Umezawa, H., Ed. Academic Press: Tokyo, 1987; pp 339–356.
(34) Hegedus, L. S.; Montgomery, J.; Narukawa, Y.; Snustad, D. C. *J. Am. Chem. Soc.* **1991**, *113*, 5784.

Scheme 3

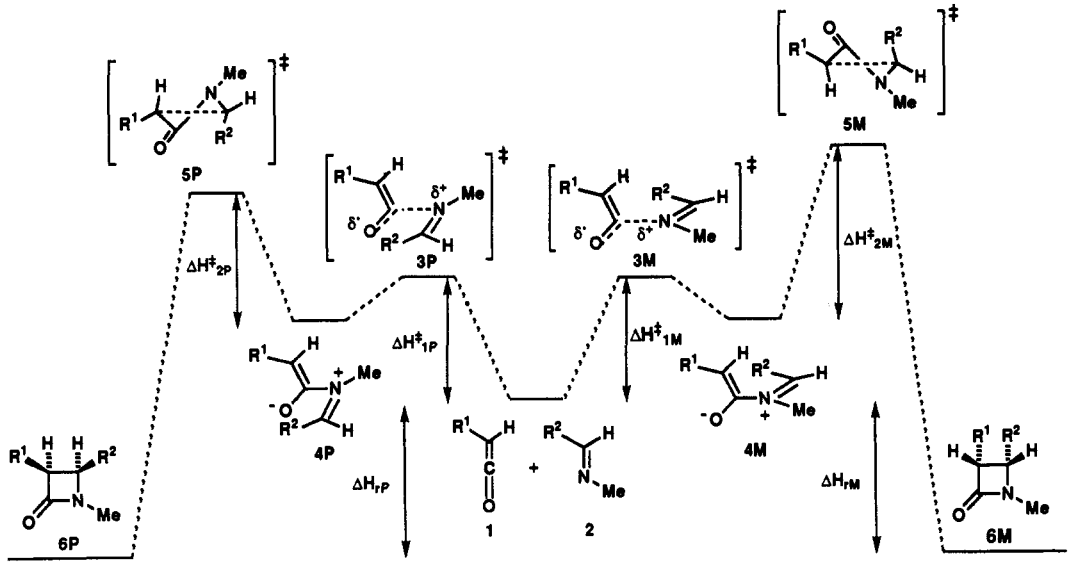

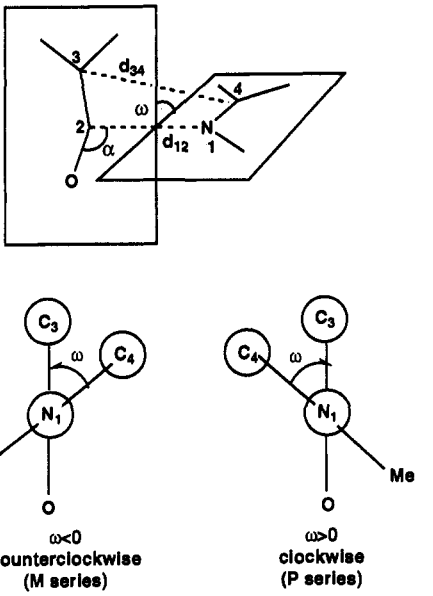

Figure 1. Graphical definition of the geometric parameters used in this study.

As it has been anticipated above, if we assume that the intermediates **4M** and **4P** are rapidly interconvertible relative to the rate of product formation, according to the Curtin–Hammett/Winstein–Holness kinetics,[36] the diastereomeric excess (de) in the formation of β-lactams **6** can be calculated by means of the following approximate expression:

$$\text{de} = \frac{|[\mathbf{6P}] - [\mathbf{6M}]|}{[\mathbf{6P}] + [\mathbf{6M}]} \approx \frac{|1 - \exp(-\Delta G_{TS2}^{\ddagger}/RT)|}{1 + \exp(-\Delta G_{TS2}^{\ddagger}/RT)} \qquad (2)$$

where $\Delta G_{TS2}^{\ddagger}$ is the difference between the standard free energies of the TSs involved in the formation of the C_3–C_4 bond:

$$\Delta G_{TS2}^{\ddagger} = \Delta G^{\circ}(\mathbf{5P}) - \Delta G^{\circ}(\mathbf{5M}) \qquad (3)$$

i.e., the theoretical de can be estimated directly from the standard free energies of the TSs **5M** and **5P**.

In order to investigate the main factors which control the stereoselectivity in the asymmetric SR, we have selected two sets of ketenes **1a–c** (Chart 1) and (*E*)-imines **2a–f** (Chart 2). The β-lactams **6Pa–g** and **6Ma–g** resulting from these reactants are depicted in the Chart 3. These choices incorporate the structural features of the most efficient approaches to the asymmetric SR

Chart 1

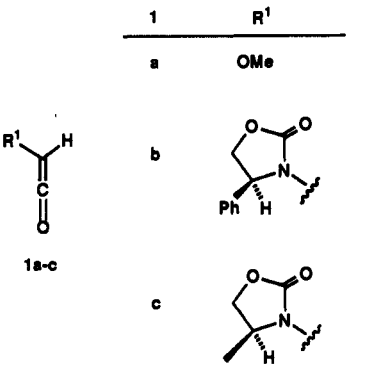

Chart 2

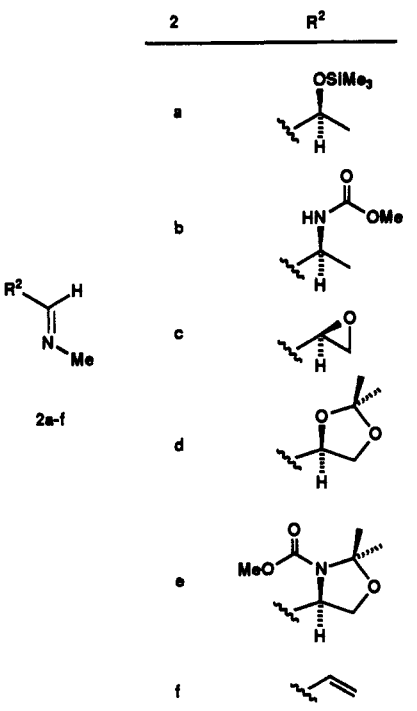

(35) (a) Houk, K. N.; Li, Y.; Evanseck, J. D. *Angew. Chem., Int. Ed. Engl.* **1992**, *32*, 682. (b) Houk, K. N. In *Strain and Its Implications in Organic Chemistry*; de Meijere, A., Bletcher, S., Eds.; Kluwer: Dordrecht, 1989.

(36) Seeman, J. I. *Chem. Rev.* **1983**, *83*, 83.

Chart 3[a]

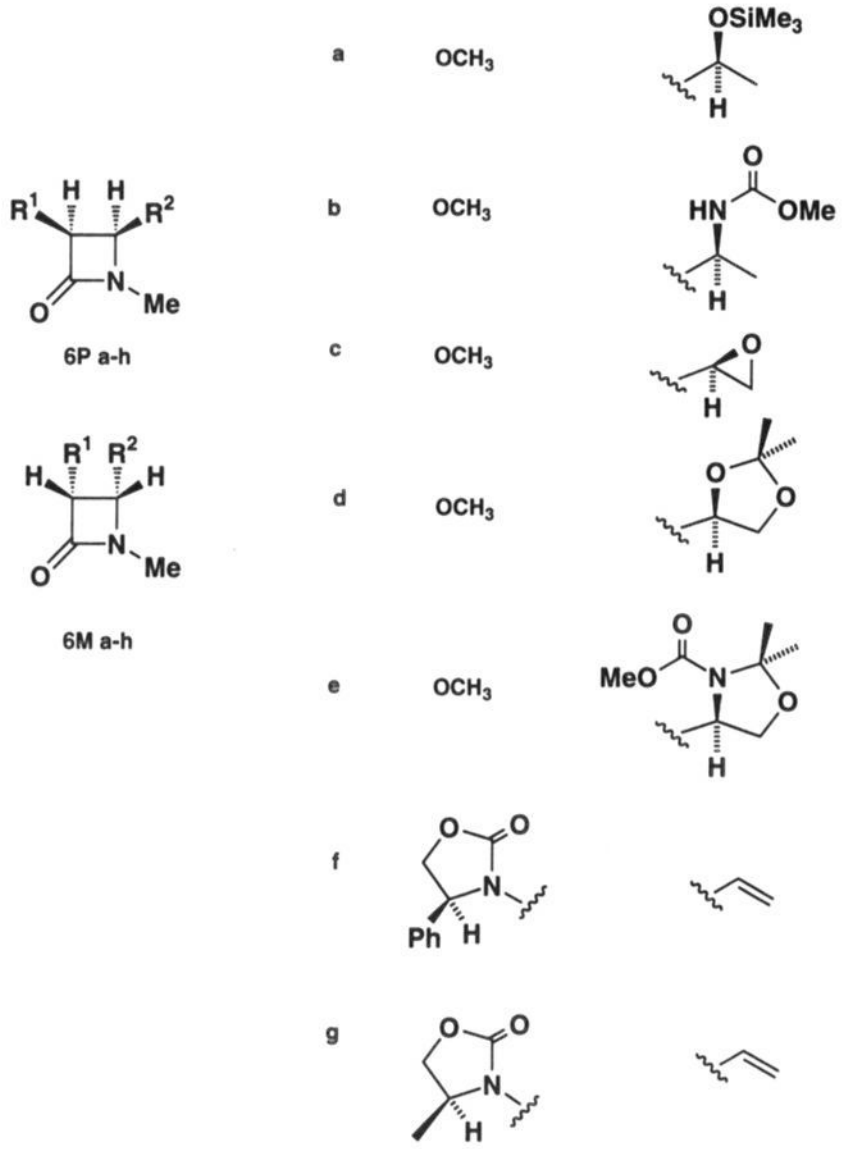

[a] The same substitution patterns correspond to the transition states **3**, **5**, and **7**, as well as the intermediates **4** (see Scheme 3).

presented in the Schemes 1 and 2. In the next sections we will present and discuss the results obtained in the SR between an achiral ketene and chiral imines, as well as between chiral ketenes and a model achiral imine.

SR between Achiral Ketenes and Chiral Imines. In order to study the reactions depicted in Scheme 1, we chose the ketene **1a** ($R^1 = OCH_3$) as a model monosubstituted achiral ketene possessing an electronegative atom in the α-position with respect to the ketene moiety and the chiral imines **2a–e**. We have collected in Table 1 of the supplementary material the values of the most relevant parameters corresponding to the TSs **3a–e**, as defined in Figure 1. In all the cases studied, two TSs **3** were found, corresponding to the **M** and **P** models, although the differences in the heats of formation ($\Delta H_f°$) between the **M** and **P** approaches are very low. This result is not surprising, since at this stage of the reaction the chiral source has no influence over the two C_3 and C_4 prochiral atoms and neither the N_1 nor the C_2 atoms are stereogenic. As a representative example, Figure 2 shows the structures and the more relevant properties of the stationary points **3Md** and **3Pd**. Inspection of Table 1 of the supplementary material reveals that there are very small differences between the **P** and **M** approaches. Thus, the N_1–C_2 distances (d_{12}) lie in the range 1.85–1.90 Å, and the α values vary between 104.8° and 106.3°. The bond indexes B_{12} between N_1 and C_2 lie in the range 0.275–0.302, whereas the B_{34} values are negligible, thus showing a complete asynchronicity in the formation of both bonds. These results reveal that the carbonyl atom of the ketene still retains a significant sp character at this stage of the reaction. As a consequence of the nucleophilic attack of the sp^2 nitrogen atom of the imines **2a–e**, the ketene fragments of the TSs **3a–e** develop a partial negative charge between –0.222 and –0.238 e (see magnitudes of $\sum q$ in the Table 1 of the supplementary material).

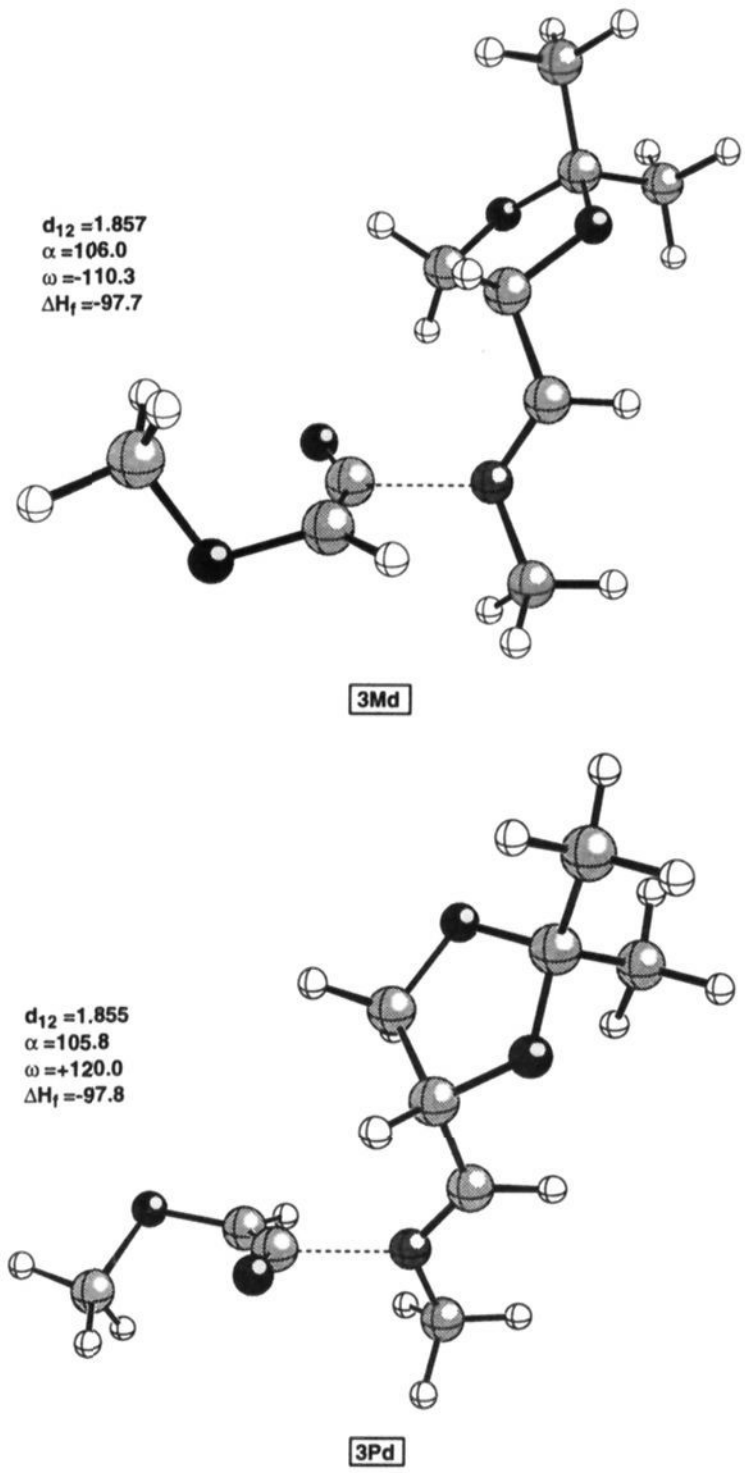

Figure 2. Computer plot of the calculated AM1 transition structures **3Md** and **3Pd**. Distances, angles, and enthalpies are given in Å, deg, and kcal/mol, respectively.

Table 1. Enthalpies of Activation and Reaction for the SR between Ketenes **1a–c** and (*E*)-Imines **2a–f**[a,b]

reaction	$\Delta H_{1M}^{\ddagger}$	$\Delta H_{1P}^{\ddagger}$	$\Delta H_{2M}^{\ddagger}$	$\Delta H_{2P}^{\ddagger}$	$\Delta H_{rM}°$	$\Delta H_{rP}°$
1a + 2a → 6a	13.5	12.8	19.2	15.7	–17.2	–21.7
1a + 2b → 6b	21.2	22.0	16.1	13.2	–12.6	–16.0
1a + 2c → 6c	19.0	18.4	13.4	12.1	–18.7	–19.0
1a + 2d → 6d	18.7	18.6	15.1	13.4	–17.2	–18.6
1a + 2e → 6e	18.8	18.9	14.9	12.9	–18.3	–18.5
1b + 2f → 6f	14.8	14.1	16.3	12.3	–14.9	–15.1
1c + 2f → 6g	14.5	13.9	13.0	12.3	–16.4	–16.1

[a] For the definition of the magnitudes, see Scheme 3. [b] All enthalpies are given in kcal/mol.

In addition, the values of the dihedral angles ω reveal, as was pointed out by Boyd *et al.*,[32] that the imine attack is not coplanar, although the steric requirements imposed by the bulky substituents of the (*E*)-imines lead to values of ω higher than 90°, as should be expected for an orthogonal approach between both partners. The calculated activation enthalpies corresponding to the first step of the SR reactions between the ketene **1a** and the (*E*)-imines **2a–e** are given in Table 1. As expected, the values for $\Delta H_{1M}^{\ddagger}$ and $\Delta H_{1P}^{\ddagger}$ lie in the range 18.7–22.0 kcal/mol, in line with our previous results on more simple substrates.[19]

The structural trends found in the TSs **3a–e** are also present in the zwitterionic intermediates **4a–e** (see Table 2 of the

supplementary material). Thus, the d_{12} values lie now in the range 1.504–1.535 Å, and the α values are closer to 120°, ranging from 112.5° to 113.7°. The bond orders B_{12} lie in the range 0.634–0.698, and the charge of the ketene fragments varies from –0.409 to –0.519 e, thus confirming the zwitterionic nature of these intermediates (see Table 2 of the supplementary material). Again, two different sets of intermediates were located, corresponding to the **M** and **P** models. Inspection of the $\Delta H_f°$ values of the **4Pa–e** and **4Ma–e** structures shown in Table 2 of the supplementary material reveals that at this stage of the SR the **P** and **M** models are isoenergetic. In addition, the rotation barriers around the N_1–C_2 bond are in the range of *ca.* 0.1–1.6 kcal/mol.[38] Therefore, the interconversion between both **P** and **M** rotamers can occur easily at room temperature, and hence, as it has been anticipated, the origin of the chiral control in the SR must be associated with the second step, *i.e.*, the conrotatory ring closure leading to the formation of the C_3–C_4 bond. As it has been depicted in the Scheme 3, the *exo* attack and the (*E*) geometry of the imine **2** lead to two possible TSs **5a–e**, both characterized by an outward disposition of the substituent at C_3, whereas the substituent at C_4 is inward according to the terminology introduced by Houk *et al.*[37] for the conrotatory thermal opening of cyclobutenes. The chief geometric and energetic characteristics of the TSs **5M** and **5P** are collected in Table 3 of the supplementary material. Inspection of the data corresponding to these TSs shows that the formation of the N_1–C_2 bond is almost completed, whereas the distances d_{34} lie in the range of 2.42–2.38 Å. Thus, the bond orders B_{12} and B_{14} lie in the intervals 0.832–0.876 and 0.353–0.401, respectively, whereas the partial charges of the ketene moiety decrease with respect to the zwitterionic intermediates **4** and vary from –0.218 to –0.297 e, very close to the values obtained for the TSs **3** (*vide supra*). The activation enthalpies corresponding to the formation of the C_3–C_4 bond have been calculated to lie in the range 12.1–19.2 kcal/mol (see Table 1), in agreement with the results previously reported for more simple systems.[19] At this stage of the chiral SR, significant differences in energy for the **5M**/**5P** pairs were found. Thus, in all the cases studied, the ΔH_f values corresponding to the TSs **5P** were found to be lower than the ΔH_f corresponding to the diastereomeric **5M** structures. To illustrate this point, Figure 3 shows a ball-and-stick representation of the TSs **5Md** and **5Pd**. Inspection of such a figure reveals, in sharp contrast with the preceding TSs **3a–e** and intermediates **4a–e**, that the shape of the structures corresponding to the **5M** and **5P** TSs is very different. Thus, the lowest energy conformation of these structures is dominated by the σ acceptor character of the C*–X bond, X being an

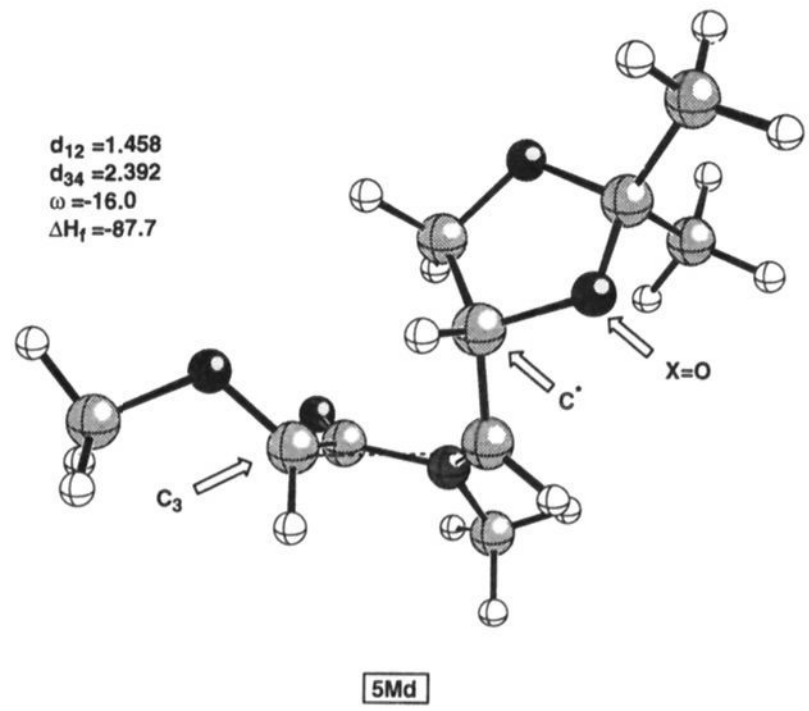

Figure 3. Computer plot of the calculated AM1 transition structures **5Md** and **5Pd**. The hollow arrows emphasize the angular and linear arrangements between the indicated atoms, respectively. Distances, angles, and enthalpies are given in Å, deg, and kcal/mol, respectively.

electronegative atom such as oxygen or nitrogen and C* a chiral carbon atom. For this conformation, the chirality of the carbon atom imposes the relative orientation of the substituent attached to the C_4 atom with respect to the forming β-lactam ring. As can be seen from Figure 3, in **5Pd** the dioxolanyl group is away with respect of the β-lactam ring. Therefore, there is not significant steric congestion, and the two-electron interaction between the $\sigma^*_{(CX)}$ orbital and the p AO of the C_3 atom (whose orientation is indicated by the hollow arrow pointing to C_3 in Figure 3) takes place efficiently through a linear arrangement of C_3 and C*–X. However, in the case of TS **5Md**, the chiral source lies over the forming β-lactam ring. Hence a linear arrangement between C_3 and the C*–X bond is not possible because of the proximity of both rings. As a consequence, the C_3···C*—X interaction takes place through a less efficient angular disposition, clearly appreciable in the structure of **5Pd**, represented in Figure 3. The final result is that **5Md** is more energetic than **5Pd**.[39] The other TSs

(37) (a) Kirmse, W.; Rondan, N. G.; Houk, K. N. *J. Am. Chem. Soc.* **1984**, *106*, 7989. (b) Houk, K. N.; Rondan, N. G. *J. Am. Chem. Soc.* **1985**, *107*, 2099. (c) Rudolf, K.; Spellmeyer, D. C.; Houk, K. N. *J. Org. Chem.* **1987**, *52*, 3708. (d) Houk, K. N.; Spellmeyer, D. C.; Jefford, Ch. W.; Rimbault, C. G.; Wang, Y.; Miller, R. D. *J. Org. Chem.* **1988**, *53*, 2125. (e) Buda, A. B.; Wang, Y.; Houk, K. N. *J. Org. Chem.* **1989**, *54*, 2264. (f) Jefford, Ch. W.; Bernardinelli, G.; Wang, Y.; Spellmeyer, D. C.; Buda, A.; Houk, K. N. *J. Am. Chem. Soc.* **1992**, *114*, 1157. (g) Niwayama, S.; Houk, K. N. *Tetrahedron Lett.* **1993**, *34*, 1251.

(38) These barriers were calculated from the differences in enthalpy between the intermediates **4** and the TSs **7**, which connect the **4M** and **4P** rotamers. The saddle points **7** showed ω values of *ca.* 180° and one imaginary frequency, associated with the rotation around the N_1–C_2 bond (see Table 5 of the supplementary material).

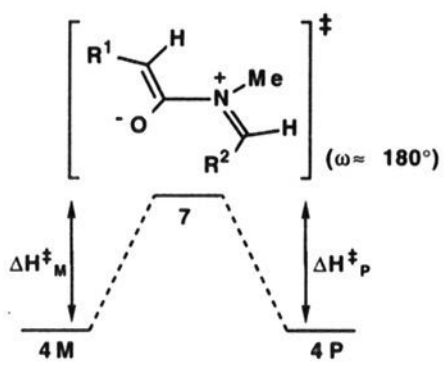

(39) From a more quantitative standpoint, an analysis of the energy partitioning (ENPART keyword) of the total energies corresponding to both TSs reveals that, although the net interaction energy between C_3 and C* (see Figure 3) is positive, in the TS **5Pd** the destabilization is 0.31 kcal/mol lower than in **5Md**, despite the fact that the distance between the two atoms is 2.680 Å for **5Pd** and 2.726 Å for **5Md**. This accounts for *ca.* the 21% of the difference in energy between both TSs. The rest corresponds to the higher repulsive interaction between the dioxolane and the β-lactam rings in **5Md**.

Table 2. Calculated and Observed Diastereomeric Excesses in the SR between Ketenes **1a–c** and (*E*)-Imines **2a–f**[a,b]

reaction	$-\Delta H_{TS}^{\ddagger}$	$-\Delta G_{TS}^{\ddagger}$	de (%) calcd	de (%) obsd (ref)
1a + 2a → 6a	4.7	6.4	100.0	>90 (11)
1a + 2b → 6b	2.8	2.9	98.5	>95 (13b)
1a + 2c → 6c	1.9	1.3	79.0	80–90 (12)
1a + 2d → 6d	1.5	1.4	83.1	>95 (9, 10)
1a + 2e → 6e	1.7	2.2	95.5	>95 (13a)
1b + 2f → 6f	4.9	3.7	99.6	99 (14–16)
1c + 2f → 6g	1.8	1.6	87.2	90 (18)

[a] The magnitudes are defined in eqs 2 and 3. [b] All energies are given in kcal/mol. The standard free energies have been computed at 298 K.

5Pa–e and **5Ma–e** showed similar characteristics, and in all cases studied the **5P** structures were found to be less energetic than the **5M** ones, the $\Delta H_{TS}^{\ddagger}$ values being in the range of 1.5–4.7 kcal/mol (see Table 2). In addition, the $\Delta G_{TS}^{\ddagger}$ values at 298 K were also calculated and found to be in the range 1.3–6.4 kcal/mol. The calculated diastereomeric excesses according to eqs 2 and 3 are also collected in Table 2 and lie in the range of 79.0–100.0%. The main discrepancy found between calculated and observed des corresponds to the interaction between ketene **1a** and the Hubschwerlen–Schmid imine **2d**. However, these values agree reasonably well with the experimental ones. In particular, our model reproduces correctly the relatively lower stereocontrol observed in the SR between achiral ketenes and the homochiral Evans–Williams epoxy imines.

Finally, we have also calculated the structures and the energies of the β-lactams **6Ma–e** and **6Pa–e**, and the results obtained are collected in the Table 4 of the supplementary material. The main features of the AM1 geometries obtained for diverse β-lactams have been commented upon by us[19] and by Frau *et al.*[40] The results obtained for the β-lactams **6a–e** are in line with the previously reported ones. Thus, the calculated N_1–C_2 bond distances are found to be of 1.395–1.414 Å, whereas the experimental values[41] are of *ca.* 1.36 Å. This discrepancy is consistent with the underestimation of the amide resonance in the β-lactam ring. We have found that in all the cases studied, the **6Pa–e** products are more stable than the **6Ma–e** isomers. Thus, in this kind of reaction, the kinetically favored β-lactams **6Pa–e** are predicted to be also thermodynamically more stable. It is noteworthy that in the case of the β-lactam **6Pe** (see Figure 1 of the supplementary material), the more stable conformation predicted by the AM1 method agrees with the X-ray structure obtained in a closely related compound.[13b]

SR between Chiral Ketenes and Achiral Imines. The next step of our study was to elucidate the origin of the chiral control in the SR between ketenes of type **1b,c** and the (*E*)-*N*-methylvinylideneamine **2f**, selected as a model achiral imine. It is interesting to note that, whereas there is a reasonable model[42] for the chiral control in the aldol reaction of enolates derived from chiral 2-oxazolidinones, no previous discussion on the origin of the high chiral control of the Evans–Sjögren ketenes in the SR has been published to date.

First, we calculated the structure and the energy of the classical Evans–Sjögren ketene **1b**, derived from (*S*)-phenylglycine. Two local minima were found and are shown in Figure 4. It is worth noting that the oxazolidine ring is not coplanr with the plane defined by the valences of the sp^2 carbon at the internal terminus of the ketene. The same situation was found in the ketene **1c**. The explanation for this result can be found by taking into account the fact that the frontier molecular orbitals (FMOs) of a ketene

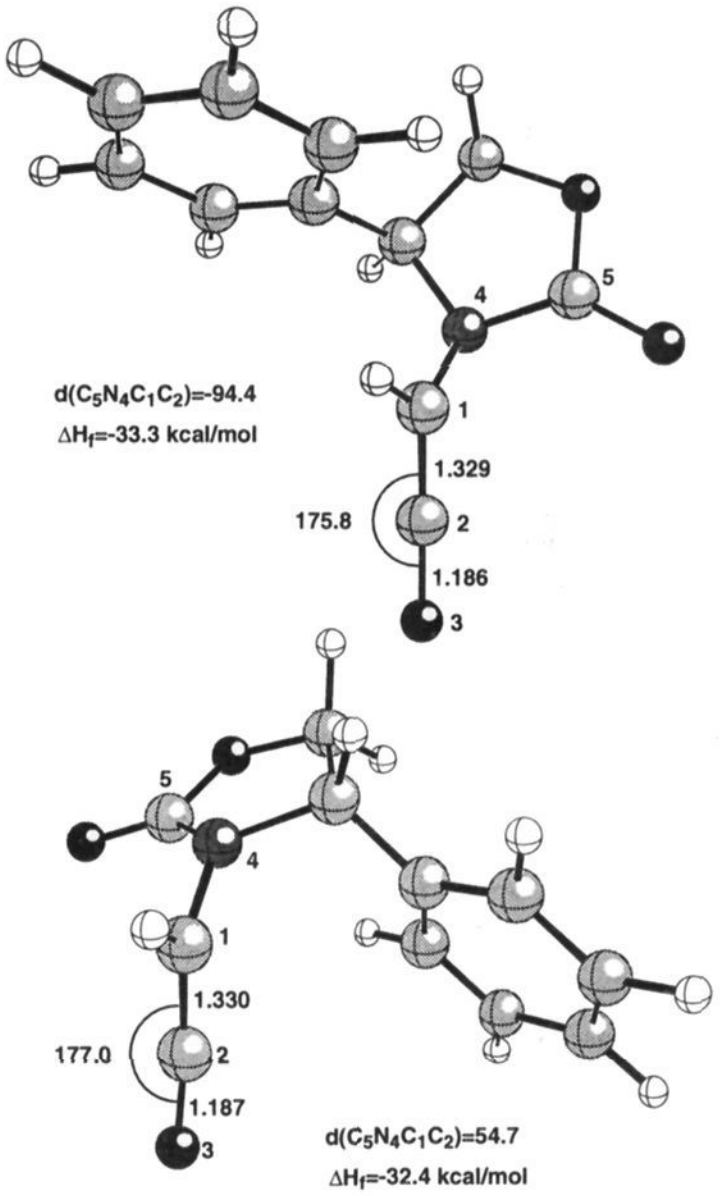

Figure 4. Computer plot of the two minimum energy conformations of the Evans–Sjögren ketene **1b** as predicted by the AM1 method. Distances and angles are given in Å and deg, respectively.

lie on orthogonal planes.[43] Thus, Figure 2 of the supplementary material shows that for the coplanar conformation A, there is a repulsive, four-electron interaction between the lone pair of the nitrogen and the HOMO of the ketene. By contrast, for the orthogonal conformation B, there is a stabilizing, two-electron interaction between the lone pair of the nitrogen and the LUMO of the ketene. Therefore, the conformation A is expected to be of higher energy.[45] High-level *ab initio* calculations on the more simple hydroxy ketene and amino ketene have yielded similar results.[46] It is interesting to note that AM1 predicts that the bond angle C_1–C_2–O_3 in the ketene **1b** (see Figure 4) is lower than 180.0°, and therefore the carbonyl oxygen of the ketene is bent away from the nitrogen. Similar results have been obtained for all the ketenes **1a–c**. Tidwell *et al.*[46] have reported the same angular distortion in their high-level *ab initio* study on ketenes. These authors and Brown *et al.*[47] have attributed this bending to electrostatic repulsion between the electronegative atom and the carbonyl π bond.

(40) (a) Frau, J.; Coll, M.; Donoso, J.; Muñoz, F.; Garcia-Blanco, F. *J. Mol. Struct. (THEOCHEM)* **1991**, *231*, 109. (b) Frau, J.; Donoso, J.; Muñoz, F.; Garcia-Blanco, F. *J. Mol. Struct. (THEOCHEM)* **1991**, *251*, 205.

(41) (a) Yang, B. Q.; Seiler, P.; Dunitz, J. D. *Acta Crystallogr., Sect. C* **1987**, *43*, 567. (b) *Physical Methods in Heterocyclic Chemistry*; Gupta, R. R., Ed.; Wiley: New York, 1984; pp 340–347 and references therein.

(42) See, for example: Evans, D. A. *Aldrichim. Acta* **1982**, *15*, 23.

(43) Saebo, S.; Radom, L. *J. Mol. Struct.* **1982**, *89*, 227.

(44) (a) *A Pictorial Approach to Molecular Structure and Reactivity*; Hout, R. F., Jr., Pietro, W. J., Hehre, W. J., Eds.; John Wiley & Sons: New York, 1984; pp 208–209. (b) Seikaly, H. R.; Tidwell, T. T. *Tetrahedron* **1986**, *42*, 2587. (c) Tidwell, T. T. *Acc. Chem. Res.* **1990**, *23*, 273.

(45) It is interesting to note that in the more stable conformer of **1b** the dihedral angle C_5–N_4–C_1–C_2 approaches to the "ideal" value of 90°, whereas in the case of the less stable conformer this dihedral angle is lower. The reason for this distortion is that the phenyl group interacts unfavorably with the ketene moiety, as an analysis of the bicentric terms corresponding to the energy partitioning for both conformers reveals. It is found that the distortion minimizes this destabilizing interaction. Calculations on related achiral ketenes give dihedral angles close to 90°.

(46) Gong, L.; McAllister, M. A.; Tidwell, T. T. *J. Am. Chem. Soc.* **1991**, *113*, 6021.

(47) Brown, R. D.; Godfrey, P. D.; Wiedenmann, K. H. *J. Mol. Spectrosc.* **1989**, *139*, 241.

As a representative example, Figure 3 of the supplementary material shows a ball-and-stick drawing of the TSs **3Mf** and **3Pf**. In general, the geometric features of these TSs **3f,g** are similar to those obtained for their **3a–e** partners (see Table 1 of the supplementary material). Thus, the N_1–C_2 distances were found to be in the range 1.873–1.904 Å, and the α values are of *ca.* 105° for both rotamers. However, the ω values are lower than those for the examples discussed in the preceding section. Again, in all the cases studied, two **P** and **M** structures were found. As was commented upon in the preceding section, the differences in energy between the **P** and **M** models for the TSs **4f,g** are low, the **P** approach being slightly less energetic. The same trend has been found for the intermediates **4Pf,g** and **4Mf,g** (see Table 2 of the supplementary material). The interconversion barrier between both rotamers is again low,[38] although slightly higher than in the preceding case (see Table 5 of the supplementary material). Therefore, as in the case studied in the preceding section, the first step of the SR between chiral ketenes and achiral imines will not determine the observed stereochemical course of the whole reaction.

The explanation of the high stereocontrol observed must lie again in the difference in energy between the TSs **5Pf,g** and **5Mf,g**. As was found in the preceding section, the shapes of the TSs **5Mf,g** and **5Pf,g** are very different. The main structural features and the energies of these structures are collected in Table 3 of the supplementary material. In Figure 5, the TSs **5Pf** and **5Mf**, leading to the *cis*-(3*S*,4*R*)-β-lactam **6Pf** and to the *cis*-(3*R*,4*S*)-β-lactam **6Mf**, respectively, are shown. Note that the conformation of the vinyl group leads to a maximum stabilization of the π acceptor with the p AO of the C_3 atom. In addition, in both TSs the (*S*)-4-phenyloxazolidinyl ring is not coplanar with the β-lactam ring in formation, and the two carbonyl groups are as distant as possible. Therefore, the only difference between the two TSs lies in the relative disposition of the phenyl group. Thus, in **5Pf** this group is away from the β-lactam ring in formation, whereas in **5Mf** the phenyl group is relatively close to the 2-azetidinone ring. An energy partitioning calculation for **5Mf** and **5Pf** reveals that the interaction energy between the phenyl group and the carbonyl oxygen of the β-lactam ring is of +2.5 kcal/mol for **5Mf** (mainly Coulombic repulsion), whereas for **5Pf** it is of only +0.5 kcal/mol. This electrostatic repulsion accounts for 41% of the difference in energy between both TSs. The rest of this difference corresponds to the interaction between the phenyl group and the remaining atoms of the β-lactam ring, as well as the vinyl group at the C_4 position. Therefore, the *cis*-(3*S*,4*R*)-β-lactam **6Pf** will be obtained as the major isomer. The same results were observed in the case of the TSs **5g**. Inspection of the data collected in Table 2 reveals that the diastereomeric excesses obtained according to our calculations are again in good agreement with the observed ones. It is noteworthy that the computed $\Delta G_{TS}^{\ddagger}$ differences are smaller than the $\Delta H_{TS}^{\ddagger}$ ones. Thus, the entropic relationship between the TSs **5Pf,g** and **5Mf,g** is the reverse of the enthalpic term. In fair agreement with available experimental data,[18] a methyl group present in the chiral source is enough to induce a good stereoselection. In addition, our calculations explain why a chiral center located at the 4-position of an imidazolidine ring (see Scheme 2, entries c and d) has no influence on the observed stereochemical outcome.[18] In Figure 7, the hollow arrows indicate that the position of this hypothetical chiral center lies away from the two prochiral C_3 and C_4 atoms. Therefore, the sense of induction is completely governed by the chiral center contiguous with the nitrogen attached to the C_3 atom of the β-lactam ring.

The structures of the β-lactams (3*S*,4*R*)-**6Pf,g** and (3*R*,4*S*)-**6Mf,g** are reported in the Table 4 of the supplementary material. The general features of these reaction products do not differ substantially from the structures of β-lactams previously reported by us[19] and therefore will not be discussed here. However, it is interesting to note that the kinetic products, the (3*S*,4*R*)-**6Pf,g** isomers, are predicted to be almost isoenergetic with respect to the minor isomers (3*R*,4*S*)-**6Mf,g**, the corresponding $\Delta H_r°$ values being very similar (see Table 1).

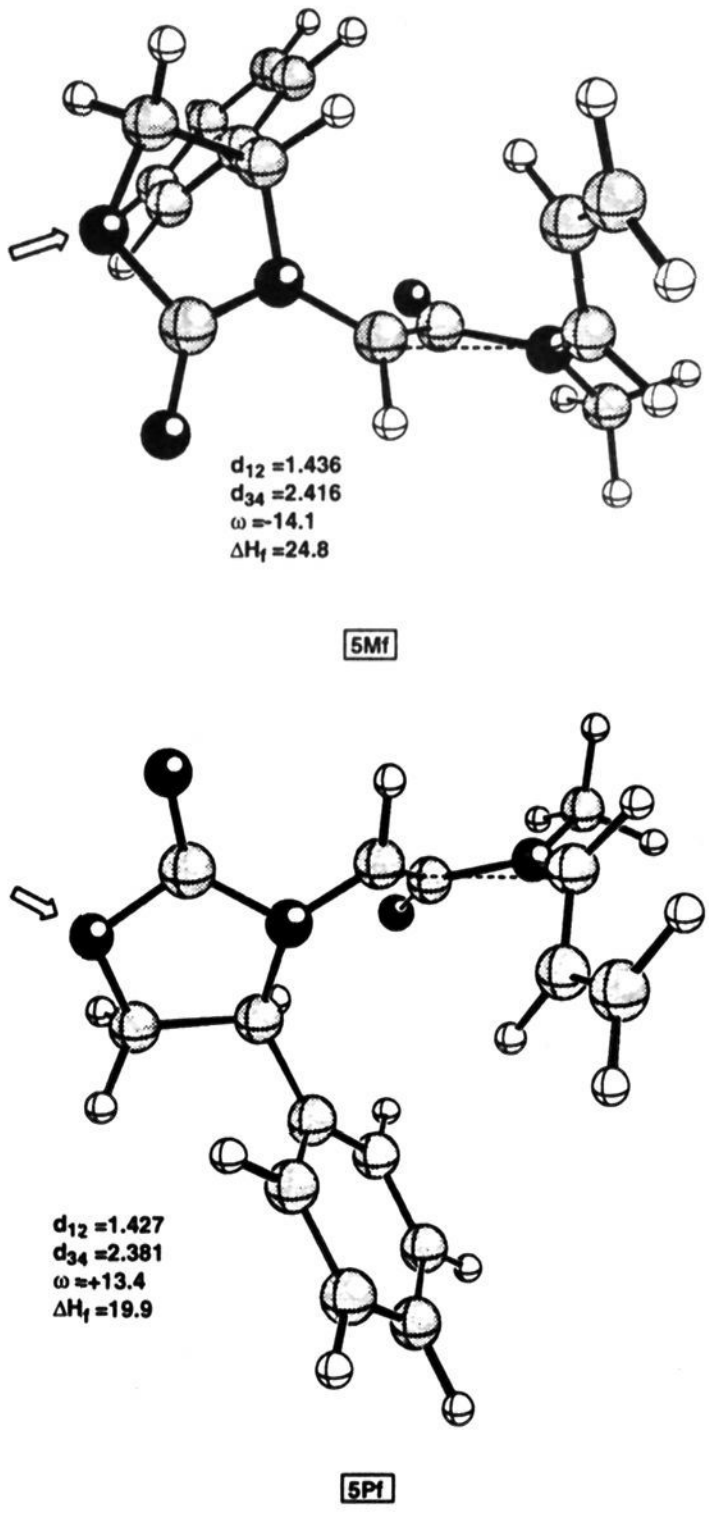

Figure 5. Computer plot of the calculated AM1 transition states **5Mf**, leading to the minor estereoisomer *cis*-(3*R*,4*S*)-**6Pf** and -**5Pf**, leading to the major *cis*-(3*S*,4*R*)-β-lactam **6Pf**. The hollow arrows indicate the position of a hypothetical substituent incorporated into an imidazolidine ring (see text). Distances, angles, and enthalpies are given in A, deg, and kcal/mol, respectively.

Conclusions

The following conclusions can be drawn from the results of the AM1 calculations above: (a) the chiral control in the SR between ketenes and imines to form *cis*-β-lactams depends upon the second step of the reaction, *i.e.*, the formation of the C_3–C_4 bond; (b) the stereochemistry observed in the SR between achiral ketenes and chiral imines derived from enantiomerically pure α-amino or α-alkoxy aldehydes is governed by the interaction in the second TS between the AO of the C_3 atom and the C*–X σ acceptor, C* being a chiral carbon and X an electronegative atom; (c) the stereochemistry observed in the SR between chiral Evans–Sjögren ketenes and achiral imines is also related to the second TS and is governed by the relative orientation of the group in the α-position to the nitrogen attached to the C_3 atom; (d) the calculated diastereomeric excesses compare well with the observed ones.

Therefore, in our opinion, the models reported in this work could be useful for prediction purposes in synthetic research in this area.[48]

Acknowledgment. The present work was supported by Universidad del País Vasco/Euskal Herriko Unibertsitatea (Projects UPV 203.215-E081/90 and UPV 170.215-EB043/92). Time allocation for calculations, performed on a CONVEX C-3820 supercomputer, was generously provided by Basque Country Supercomputer Center. We thank Ms. Teresa Taubmann for technical assistance.

(48) Recently, two new papers related to experimental results on the asymmetric SR between achiral ketenes and chiral imines have appeared; see: (a) Alcaide, B.; Martín-Cantalejo, Y.; Pérez-Castells, J.; Rodríguez-López, J.; Sierra, M. A.; Monge, A.; Pérez-García, V. *J. Org. Chem.* **1992**, 57, 5921. (b) Jayaraman, M.; Deshmukh, A. R. A. S.; Bhawal, B. M. *Synlett* **1992**, 749. In the former paper, the relative configurations (3*S**,4*R**,3′*R**,4′*S**) and (3*S**,4*S**,3′*R**,4′*S**) observed agreed with the stereochemical course of the SR explained by our model. In the latter paper, the relatively low diastereomeric excesses obtained (30%–80%) in the SR between achiral ketenes and imines derived from a homochiral aldehyde can be explained by the presence of a π acceptor attached to the C_4 atom instead of using a C*–X σ acceptor.

Supplementary Material Available: Tables listing the more relevant data of the stationary points **4–7a–g** (for both the **M** and **P** approaches), Cartesian coordinates of all the structures discussed in this work, computer plots of the structures **6Pe**, **3Mf**, and **3Pf**, and a diagram showing the orbital interactions in monosubstituted amino ketenes (21 pages). This material is contained in many libraries on microfiche, immediately follows this article in the microfilm version of the journal, and can be ordered from the ACS; see any current masthead page for ordering information.